Optimized Path Planning for USVs under Ocean Currents

Preprint · July 2023

DOI: 10.48550/arXiv.2307.03355

4 authors, including:

Behzad Akbari
Nipissing University
10 PUBLICATIONS **37** CITATIONS

SEE PROFILE

Ya-Jun Pan
Dalhousie University
185 PUBLICATIONS **3,689** CITATIONS

SEE PROFILE

Optimized Path Planning for USVs under Ocean Currents

Behzad Akbari, *Member, IEEE*, Ya-Jun Pan, *Senior Member, IEEE*, Shiwei Liu, and Tianye Wang

***Abstract* — The proposed work focuses on the path planning for Unmanned Surface Vehicles (USVs) in the ocean enviroment, taking into account various spatiotemporal factors such as ocean currents and other energy consumption factors. The paper proposes the use of Gaussian Process Motion Planning (GPMP2), a Bayesian optimization method that has shown promising results in continuous and nonlinear path planning algorithms. The proposed work improves GPMP2 by incorporating a new spatiotemporal factor for tracking and predicting ocean currents using a spatiotemporal Bayesian inference. The algorithm is applied to the USV path planning and is shown to optimize for smoothness, obstacle avoidance, and ocean currents in a challenging environment. The work is relevant for practical applications in ocean scenarios where an optimal path planning for USVs is essential for minimizing costs and optimizing performance.**

***Index Terms*—Gaussian process inference, Gaussian process motion planning, Factor graph optimization, Energy consumption factors, USV.**

I. Introduction

An Unmanned Surface Vehicle (USV) is a self-operating watercraft that plays a significant role in various marine applications, including military operations, surveillance, and search and rescue missions. Path planning is a crucial responsibility of an autonomous USV to ensure the success of the mission while minimizing energy consumption. To navigate effectively in a marine environment, a USV requires a global planner to establish the initial path and a local planner to manage any real-time events that may occur. The global planner typically generates the initial path by utilizing prior information on static geographic features and meteorological data. The global path can be computed in a centralized way and used as the initial path before starting the mission. However, as the USV begins interacting with its surroundings, a local planner must handle any uncertainties and update the initial path based on dynamic events and constraints. The local planner must consider factors such as collision avoidance and energy consumption, which vary over time. The initial global path can be computed centrally and utilized at the beginning of the mission. Still, the local planner must adapt to changing conditions and update the path in real time to ensure safe and efficient navigation

Despite the increasing interest in the USV path planning, significant challenges remain, including the need to consider realistic environmental impacts such as winds and surface currents. Furthermore, only a minority of algorithms take these environmental characteristics into account and fail to consider their spatiotemporal properties. Several algorithms have recently been developed to address these challenges, including Gaussian Process Motion Planning (GPMP2), which can generate short and smooth paths in a large-scale or high-dimensional space. GPMP2 is non-parametric, computationally efficient, and compatible with Markov models [1] [2]. While GPMP2's capabilities make it a promising solution for path planning in various autonomous vehicles, including USVs, there is still a need for improvements to tackle complex environments like the ocean.

This study introduces an energy consumption factor specific to ocean currents within the GPMP2 algorithm. A spatiotemporal Gaussian Process model is utilized to represent the ocean current. Incorporating a spatiotemporal filter along with the energy consumption factor produces a seamless, ongoing, and adaptable path for each step, reducing the probability of collisions and energy consumption. The system's interaction and stability are enhanced by utilizing a local planner to optimize the entire trajectory in each time step. The factor graph method allows us to address intricate optimization problems like GPMP2 in real-time. This paper makes several significant contributions, including:

1) Introducing a novel spatiotemporal Gaussian process inference technique to track ocean currents throughout the trajectory in each time step, which has not been done before.
2) Utilizing the estimated ocean current vector in combination with GPMP2 to generate a path that minimizes energy consumption and ensures collision avoidance.
3) The ocean current dataset for Halifax Harbor is utilized for training the model and determining the kernel parameters and transition matrices.

II. Related Works

When it comes to planning paths for USVs, commonly employed approaches include optimization, heuristic searching, or a blend of both. One of the optimization methods commonly used is the Artificial Potential Field (APF), which generates a potential field of the environment and constraints to create a path. The destination generates global forces, while obstacles and constraints generate local repulsive forces. A multi-layered APF model that minimizes energy consumption is introduced in [3] for USV path planning. In dynamic environments, the collision risk is measured by local repulsive forces based on the distance between the USV and the closest obstacles. Wind and currents, which are external and time-varying factors, can also create collision risks. The Fast Marching Method (FMM) has been proposed in [4] [5] as a solution to generate the shortest path while considering these factors. Additionally, a variation of FMM called anisotropic fast marching (AFM) has been combined with GPMP2 and augmented with factors for wind or ocean currents in [6]. The AFM method expands upon the capabilities of the FMM by accommodating

B. Akbari and Y.J. Pan are with the Department of Mechanical Engineering, Dalhaousie University, Halifax, NS, Canada, B3H 4R2. (Email: bh888652@dal.ca, yajun.pan@dal.ca). Shiwei Liu and Tianye Wang are with Marine Thinking, 1096 Marginal Road, Halifax, NS B3H 4N4. (Email: shiwei.liu@marinethinking.com, tianye.wang@marinethinking.com).

anisotropic media, wherein the speed of the wavefront can vary across different directions. This extension proves particularly advantageous in the path planning where the medium involves direction-dependent factors, such as external forces impacting the movement. Heuristic methods commonly employed in the USV path planning, include frequently used algorithms such as Ant Colony Optimization (ACO), A-star (A*), and Dijkstra's algorithm [7] [8]. Sampling-based planning methods offer an alternative solution to graph-based global planners and do not require a grid map to initialize the state space before the planning phase begins [9]. Two types of sampling-based algorithms include multi-query planners, such as the Probabilistic Road Map (PRM)) [10], and single-query planners, such as the Rapidly-exploring Random Tree (RRT) [11]. The RRT algorithm incrementally builds a tree to fill the entire search space with randomly sampled points, making it an effective tool for finding solutions in high-dimensional spaces. However, it can generate low-quality paths, and the final path can be quite different if the search process is allowed to repeat under the same conditions. To address these issues, the RRT* algorithm was proposed, which incrementally reconnects the tree around a new node and its neighboring nodes to improve the quality of the solution [12]. In our application, we have prior knowledge of the start and goal points, and the computational resources used in the RRT* algorithm are efficient [13]. Consequently, in our algorithm, the RRT* algorithm was employed to obtain the initial path.

Table I: Abbreviations adopted in this manuscript

Abbreviation	Description
USV	Unmanned Surface Vehicle
GP	Gaussian Process [14]
GPMP	Gaussian Process Motion Planning [15] [16]
MRPP	Multi-Robot Path Planning
APF	Artificial Potential Field
FMM	Fast Marching Method
ACO	Ant Colony Optimisation
MAP	Maximum A Posteriori
LTV-SDE	Linear Time-varying Stochastic Differential Equation
PRM	Probabilistic Road Map
RRT	Rapidly-exploring Random Tree [11]
BFGS	Broyden-Fletcher-Goldfarb-Shanno
AFM	Anisotropic Fast Marching
GPGN	Gaussian process Gauss-Newton

III. USV Trajectory Optimization

The smooth nature of ocean phenomena motivates us to utilize Gaussian process function optimization. A GP can be considered a generalization of a Gaussian random variable in a continuous-time domain [17]. Instead of a mean vector and a covariance matrix, a GP state $x(t)$, is described by a mean function, $\mu(t)$, and a covariance or kernel function, $K(t,t')$. The system model is described as follows:

$$\mathbf{x}(t) \sim GP\big(\boldsymbol{\mu}(t), \mathbf{K}(t,t')\big), \tag{1}$$

$$z_{i,e_l} = h_{i,e_l}\big(x(t_i)\big) + w_{i,e_l},\ w_{i,e_l} \sim N\left(0, \Sigma_{i,e_l}\right). \quad 1 \le l \le M, \tag{2}$$

For l different events, measurements z_{i,e_l} for an event e_l at time t_i are obtained by the (generally nonlinear) discrete-time measurement function $h_{i,e_l}(.)$ and assumed to be corrupted by zero-mean Gaussian noise with covariance Σ_{i,e_l}. Evaluating these expressions at discrete instants of time results in a joint Gaussian random variable. Usually a GP function can be represented by a small number of states n_s and their interpolations. An efficient gradient-based optimization algorithm can be used to compute the GP interpolation. Formally, trajectory optimization aims to determine the optimal trajectory from all feasible trajectories while satisfying all events and minimizing event's cost. GP regression is performed by a maximum a posteriori (MAP) inference, where the most likely trajectory is the mean of the posterior distribution conditioned on the events and corresponding measurements. The MAP estimate of the trajectory can be computed through the Gaussian process Gauss-Newton (GPGN) [18]. To define the objective function for trajectory $\mathbf{x}$, we assume that there are M observations between time t_1 to t_M.

$$\mathbf{x} = \begin{bmatrix} x(t_1), \dot{x}(t_1), \\ \vdots \\ x(t_M), \dot{x}(t_M) \end{bmatrix},\ \boldsymbol{\mu} = \begin{bmatrix} \mu(t_1) \\ \vdots \\ \mu(t_M) \end{bmatrix}, \mathbf{K} = \left[K(t_i, t_j)\right]|_{ij},\ 1 \le i,j \le M, \tag{3}$$

$$\boldsymbol{z}_{e_l} = \begin{bmatrix} z(t_1) \\ \vdots \\ z(t_M) \end{bmatrix},\ \boldsymbol{h}(\boldsymbol{x}) = \begin{bmatrix} h_1(t_1) \\ \vdots \\ h_M(t_M) \end{bmatrix}, \boldsymbol{\Sigma} = diag[\Sigma_1 \dots \Sigma_M]. \tag{4}$$

A posterior function for state $\mathbf{x}$ for measurement $\mathbf{Z}$ can be written as $\mathrm{P}(\mathbf{x}|\mathbf{z})$. The optimal trajectory coming from the MAP estimation of the posterior function as:

$$\mathbf{x}^* = \underset{x}{\operatorname{argmax}}\ \mathrm{P}(\mathbf{x}|\mathbf{z}). \tag{5}$$

The proportion of posterior distribution of $\mathbf{x}$ given $\mathbf{z}$ can be derived from the prior $\mathrm{P}(\mathbf{x})$ and likelihood $\mathrm{L}(\mathbf{z}|\mathbf{x})$ by Bayes rule as:

$$\mathrm{P}(\mathbf{x}|\mathbf{z}) \propto \mathrm{P}(\mathbf{x})\mathrm{L}(\mathbf{z}|\mathbf{x}). \tag{6}$$

This formula will be represented as the product of a series of factors [19],

$$\mathrm{P}(\mathbf{x}|\mathbf{z}) \propto \mathrm{P}(\mathbf{x})\mathrm{L}(\mathbf{z_1}|\mathbf{x}) \dots \mathrm{L}\big(\mathbf{z_{N_f-1}}|\mathbf{x}\big) \propto \prod_{n_f=1}^{N_f} f_{n_f}\left(\mathbf{x}_{\boldsymbol{n_f}}\right), \tag{7}$$

where f_{n_f} are n_f events of factors on state subsets $\mathbf{x}_{n_f}$. In situations involving spatiotemporal measurements like ocean currents, where actual values cannot be obtained throughout a trajectory, estimated measurements known as pseudo measurements are used instead. To efficiently solve the maximum a posteriori (MAP) problem, which involves all factors, the sparsity present in the factor graph can be exploited, as shown in [19].

1) GP Markov model

Based on [19] [20], a linear time-varying stochastic differential equation form of a GP can be written as:

$$\dot{\mathbf{x}}(t) = \mathbf{A}(t)\mathbf{x}(t) + \boldsymbol{\vartheta}(t) + \mathbf{F}(t)\mathbf{w}(t), \tag{8}$$

where $\dot{\mathbf{x}}(t)$ is the next vector-valued state of trajectory, $\boldsymbol{\vartheta}(t)$ is the known system control input, $\mathbf{A}(t)$ and $\mathbf{F}(t)$ are time-varying matrices of the system, and $\mathbf{w}(t)$ is generated by a white noise process. The white noise process is itself a zero-mean GP:

$$\mathbf{w}(t) \sim GP\big(0, \boldsymbol{Q_C}\delta(t - t')\big), \tag{9}$$

where $\boldsymbol{Q_C}$ is the power-spectral density matrix and $\delta\ (t - t')$ is the Dirac delta function. The solution to the initial value problem of this Linear Time-Varying Estocastic Differential Equation (LTV-SDE) is in the form of mean and covariance [20]:

$$\tilde{\boldsymbol{\mu}}(t) = \boldsymbol{\Phi}(t, t_0)\boldsymbol{\mu}_0 + \int_{t_0}^{t} \boldsymbol{\Phi}(t,s)\boldsymbol{\vartheta}(s)ds, \tag{10}$$

$$\tilde{\mathbf{K}}(t,t') = \mathbf{\Phi}(t,t_0)\mathbf{K}_0\mathbf{\Phi}(t',t_0)^T + \int_{t_0}^{\min(t,t')} \mathbf{\Phi}(t,s)\mathbf{F}(s)\boldsymbol{Q}_c\mathbf{F}(s)^T\mathbf{\Phi}(t',s)^T ds\,, \quad (11)$$

where $\mathbf{\Phi}$ is the state transition matrix, and $\boldsymbol{\mu}_0$ and $\mathbf{K}_0$ are the mean and covariance, at t_0 respectively. The Markov property of Eq.(10) results in the sparsity of the inverse kernel matrix $\mathbf{K^{-1}}$, which allows for a fast inference. Then the GP prior represents the dynamics of a system, and its proportion can be written as follows:

$$\mathrm{P}(\mathbf{x}) \propto \exp\left\{-\frac{1}{2}\| \mathbf{x}-\boldsymbol{\mu} \|^2_{\mathbf{K}}\right\}. \quad (12)$$

The likelihood function formulates constraints as events that the GP function has to obey. For example, the likelihood function of obstacle avoidance in a path planning scenario indicates the probability of being free from obstacles. All the likelihood functions need to be limited to the exponential family, given by:

$$L\left(\mathbf{x};\, e_{n_f}\right) \propto \exp\left\{-\frac{1}{2}\| h_{n_f}(\mathbf{x}) \|^2_{\Sigma_{n_f}}\right\}, \quad (13)$$

where $h_{n_f}(\boldsymbol{x})$ is a vector-valued cost function for an event n_f and $\|.\|^2_{\boldsymbol{\Sigma}n_f}$ is the Mahalanobis distance with hyper parameters (covariance) $\boldsymbol{\Sigma}_{n_f}$.

2) MAP inference

Using Eqns. (7), (12), and (13), after operating $-\log(.)$ and converting $argmax$ to $argmin$, the MAP posterior estimation can be formulated as

$$\mathbf{x}^* = \underset{\mathbf{x}}{\operatorname{argmin}}\{ \frac{1}{2}\| \mathbf{x}-\boldsymbol{\mu} \|^2_{\mathbf{K}} + \frac{1}{2}\| h_2(\mathbf{x}) \|^2_{\boldsymbol{\Sigma}_2} + \cdots + \| h_{n_f}(\mathbf{x}) \|^2_{\boldsymbol{\Sigma}_{n_f}} \}, \quad (14)$$

which is a nonlinear least square problem that can be solved by iterative algorithms such as Gauss-Newton or Levenberg-Marquardt until convergence. The corresponding linear equation is as follows:

$$\mathbf{x}^* = \underset{r}{\operatorname{argmin}} \| \boldsymbol{A}x - \boldsymbol{b} \|^2, \quad (15)$$

where $\boldsymbol{A} \in \mathbb{R}^{n_f \times n_s}$ is the measurement Jacobian consisting of n_f measurement rows and $\boldsymbol{b}$ is an n_s-dimensional vector computable similar to iSAM2 [21].

IV. Tracking the Energy Consumption Vector

Energy consumption factors are the environmental forces that affect the dynamics of a vehicle. In an ocean environment, these factors include water density, ocean currents, waves, and wind, all of which can impact a USV motion. These factors are spatiotemporal, meaning they depend on both space and time. As an illustration, the data obtained from the Halifax harbor indicates a significant fluctuation in the ocearn current within 24 hours due to the tides. The impact of these forces on a USV is heavily influenced by the angle at which they act on the vehicle, which is determined by the shape of the USV. For example, a long USV moving in the same direction as the current may experience less impact due to its reduced surface area exposed to the force, Fig.1. The likelihood of the Current can be characterized using an exponential family function, which is determined by the cost incurred by a trajectory $\mathbf{x}$ when encountering current velocities as:

$$L(\mathbf{x};\, e_c) \propto \exp\left\{-\frac{1}{2}\| h_c(\mathbf{x}) \|^2_{\Sigma_c}\right\}, \quad (16)$$

The cost function $h_c(\mathbf{x})$ for the currents with respect to the position x_i is further determined by a deviation based Hinge loss:

$$h_c(x_i) = \begin{cases} -d(x_i) + \epsilon & if\ d(x_i) > \epsilon \\ 0 & if\ d(x_i) \le \epsilon \end{cases}, \quad (17)$$

$d(x_i)$ is the deviation between the desired path and the actual trajectory and ϵ is the maximum allowed deviation. The function ensures that the loss is only incurred when the deviation exceeds the threshold. If the deviation exceeds the threshold ($d(x_i) > \epsilon$), the loss is proportional to the amount by which it exceeds the threshold. The hinge loss function penalizes the USV's trajectory when it deviates too far from the desired path due to the ocean current. The magnitude of the loss increases as the deviation surpasses the threshold. This loss function can be used as part of the GP function optimization to guide the USV toward its desired path while considering the influence of ocean currents. In our proposed paper, the deviation $d(x_i)$, for a position x_i computed based on Fig.1, by:

$$d(x_i) = (\vec{v}_a(x_i) - \vec{v}_c(x_i))C(\alpha)\ ;\ C(\alpha) \propto ||sin(\alpha)||. \quad (18)$$

Here, $\vec{v}_a(x_i)$ represents the actual velocity and $\vec{v}_c(x_i)$ denotes the current velocity in position x_i, with $C(\alpha)$ representing the magnitude proportion of the ocean current energy on the body of USV. In this particular study, a sin(.) function is utilized for $C(\alpha)$.

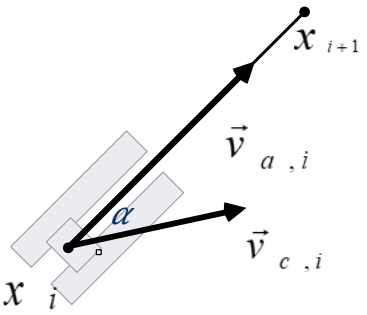

Fig. 1. The configuration of the USV and the impact of the current on its motion are described by the actual velocities $\overrightarrow{v_{a,i}}$ and the current velocity $\overrightarrow{v_{c,i}}$. These velocities refer to the two positions x_i and x_{i+1} along the trajectory.

Accurately calculating the energy consumption factor requires incorporating the current velocity into the trajectory. This section introduces a method for modeling spatiotemporal ocean currents based on a given trajectory, which enables the tracking of the energy consumption vector in both space and time. Inspired by previous extended target tracking models, our approach combines elements from [22] and [23]. Although initially designed for tracking ocean current vectors, this algorithm has the potential to be adapted for monitoring other consumption factors. Fig. 2 illustrates the concept of the energy consumption factor, represented by a state vector that indicates the opposing forces experienced by the USV as it follows its trajectory.

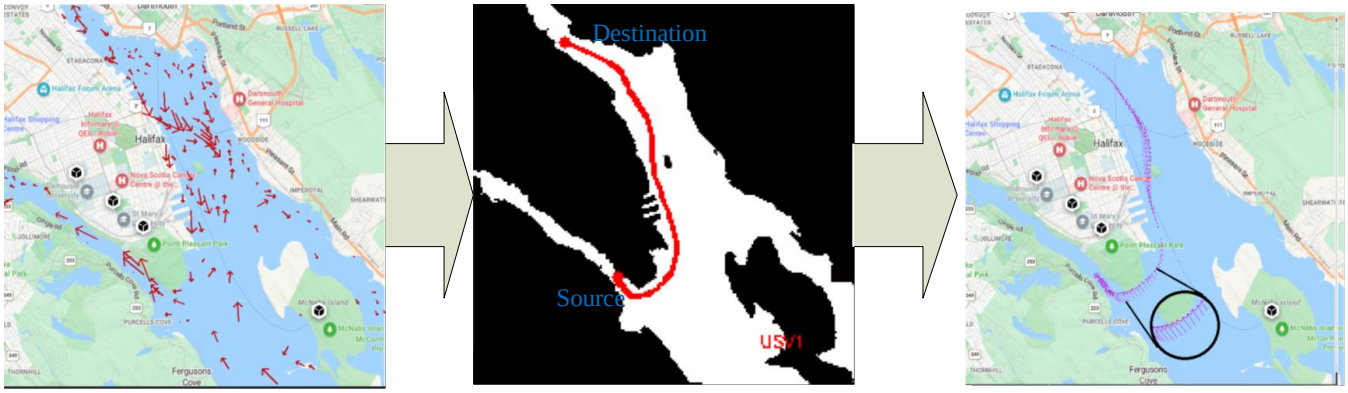

A) Observed Currents **B) Given trajectory** **C) Current vector**

Fig. 2. Using the observed measurements in subfigure A) and the previous given trajectory B), pseudo measurements are estimated for the Currents in subfigure C). The outcome of subfigure C) will be utilized to calculate the trajectory cost and find the updated optimal path.

A. *Ocean Current Model*

For a given trajectory $\boldsymbol{x}$, the ocean current $\boldsymbol{v}_c$ can be represented as a vector of the same size as the trajectory. This vector indicates the angle and magnitude of the ocean current velocity at each point along the trajectory. The Gaussian nature of ocean currents allows us to employ kernel-based spatiotemporal Gaussian process inference [22] to track the Current's state along a given trajectory in both space and time. The model includes a limited number of index points $\boldsymbol{x}$ equal to trajectory points and the latent function $\boldsymbol{v}_c(\boldsymbol{x})$ showing the angle and magnitude of Ocean currents at those points. In our Gaussian process model for simplicity, we design the dynamics of the ocean current vector as a separable kernel.

$$\kappa(x, x'; t, t') = \kappa_x(x, x')\kappa_t(t, t'), \tag{19}$$

where $\kappa(x, x'; t, t')$ is the Spatio-temporal covariance kernel, $\kappa_u(x, x')$ the spatial kernel, and $\kappa_t(t, t')$ represents the temporal covariance kernel. In this paper, the spatial kernel for two individual indexes (x, x') is considered a square exponential or Radial Basis Function (RBF) kernel as [24]:

$$\kappa(x, x')_{RBF} = \sigma^2 \exp\left(-\frac{1}{2}\frac{(x-x\prime)^2}{\ell^2}\right). \tag{20}$$

Hyperparameters of the kernel σ , ℓ are learned from the training data. For the temporal covariance kernel, we primarily use the Whittle-Matern kernel [24] will explain in section IV.C. The proposed model is converted to an equivalent state-space representation. The evolution of states is modeled as follows:

$$\mathbf{v}(\mathbf{x}, t_k) = \mathbf{F}_k \mathbf{v}(\mathbf{x}, t_{k-1}) + \mathbf{L}_k \mathbf{w}_k(\mathbf{x}), \quad \mathbf{w}_k \sim \mathcal{N}(0, \mathbf{Q}_k(\mathbf{x}, \mathbf{x}'; T_s)), \tag{21}$$

$$\mathbf{z}_k = \mathbf{H}_k \mathbf{v}(\mathbf{x}, t_k) + \upsilon_k, \quad \upsilon_k \sim \mathcal{N}(0, R). \tag{22}$$

$$\mathbf{v}(\mathbf{x}, t_k) = [[v(x_1, t_k)], [v(x_2, t_k)], \ldots, [v(x_{N^f}, t_k)]]^\top, \tag{23}$$

where $\mathbf{v}(\mathbf{x}, t_k)$ is the state of the Current in which each corresponds to N^{f} distinct index points for the trajectory, $\mathbf{x} = \{x_1, x_2, .., x_{N^f}\}$ The state transition matrix is denoted by $\mathbf{F}_k$, and $\mathbf{w}_k$ is a zero-mean white Gaussian noise with covariance $\mathbf{Q}_k$. Note that all coordinates are in Cartesian space with a single global origin. The cardinality and value of index points are related to the precision of the trajectory. To find the hyper parameters we train the model similar to a regular GP, minimizing the log marginal likelihood of measurements [25]. The training results include the kernel parameters and transition matrices.

B. *Measurement Model for Ocean Currents*

Ocean currents can be measured using a limited number of sensors around the area. Usually, the cardinality and position of the measurements are both unknown and time-varying. In addition, the measurement origin uncertainty should be considered. Considering a set of *N* distinct input positions of trajectory $\mathbf{x}^f = [x_1^f, x_2^f, \ldots x_{N^{\mathrm{f}}}^f]^\top$ for states, we want to estimate the Current states, $\mathbf{v}(\mathbf{x}^f)$, corresponding to these noisy measurements $\mathbf{z}$. The pseudo measurements corresponding to index points $\mathbf{x}_k$ (as in Fig.2.C)) is given by:

$$\boldsymbol{z}_k(\mathbf{x}_k) = \mathbf{H}_k^f(\mathbf{x}_{\mathrm{k}})\mathbf{v}_{\mathrm{k}} + \upsilon_k, \quad \upsilon_{\boldsymbol{k}} \sim \mathcal{N}(0, \mathbf{R}_k^f), \tag{24}$$

where $\mathbf{H}_k^f(\mathbf{x}_{\mathrm{k}})$ is a measurement transition matrix and $\upsilon_{\boldsymbol{k}}$ is the zero-mean Gaussian measurement noise.

The measurement likelihood is given for the measurements according to the joint distribution probability density of GP as Eqns.(23) and (24).

$$p(\boldsymbol{z}_k|\mathbf{v}_{\mathrm{k}}) \sim \mathcal{N}\left(\boldsymbol{z}_k; \mathbf{H}_k^f(\mathbf{x}_{\mathrm{k}})\mathbf{v}_{\mathbf{k}}, \mathbf{R}_k^f(\mathbf{x}_{\mathrm{k}})\right). \tag{25}$$

The implementation of the measurement transition matrix $\mathbf{H}_k^f$ and measurement covariance $\mathbf{R}_k^f$ is derived from:

$$\mathbf{H}_k^f(\mathbf{x}_{\mathrm{k}}) = (K(\mathbf{x}_k, \mathbf{x}^f))[K(\mathbf{x}^f, \mathbf{x}^f)]^{-1}, \tag{26}$$

$$\mathbf{R}_k^f(\mathbf{x}_{\mathrm{k}}) = \left(K(\mathbf{x}_k, \mathbf{x}_k)\right) + R - \left(K(\mathbf{x}_k, \mathbf{x}^f)\right)[K(\mathbf{x}^f, \mathbf{x}^f)]^{-1}\left(K(\mathbf{x}^f, \mathbf{x}_k)\right). \tag{27}$$

Based on the Current model and the measurement model discussed above, we can predict unobserved values of the Current $\mathbf{v}_d(\mathbf{x}^f)$ at index points $\mathbf{x}^f$ using observed measurements.

C. *Ocean Current Inference*

The majority of GP kernels, including the Current kernels, can be expressed using a straightforward and practical form of the State-Space Differential Equation (SDE), which is linear and time-invariant [24]. By using this model and a recursive Kalman filter, we can estimate the state and

covariance in a linear manner at each time step. In order to determine the target association, we utilize a Nearest Neighbor algorithm. The overall recursion for tracking the current vector can be reformulated as Fig.3 and Algorithm 1.

Temporal Covariance Kernel: In our application, we also used the Matern covariance function for the temporal part. We considered $\nu = 3/2$, with a continuous and once differentiable process. In this case, the covariance function is simplified to Eq. (25):

$$\kappa_t(\tau)_{\frac{3}{2}} = \sigma^2\left(1+\frac{\sqrt{3}\tau}{l}\right)exp\left(-\frac{\sqrt{3}\tau}{l}\right). \tag{28}$$

The continuous system matrix and the noise effect vector of the corresponding state-space model are derived as follows:

$$\boldsymbol{\mathcal{A}_t} = \begin{bmatrix} 0 & 1 \\ -\lambda^2 & -2\lambda \end{bmatrix}, \quad \mathbf{L}_t = \begin{bmatrix} 0 \\ 1 \end{bmatrix}, \tag{29}$$
$$\mathbf{P}_\infty = \mathbf{P}_0 = \begin{bmatrix} \sigma^2 & 0 \\ 0 & \lambda^2\sigma^2 \end{bmatrix},$$

where $\lambda = \frac{\sqrt{3}\tau}{l}$ and the spectral density of the Gaussian white process noise $w(t)$ is $\mathbf{Q}_c = 4\lambda^3\sigma^2$. The measurement model matrix is $\mathbf{H} = [1\ \ 0]$. The state of a target i can be defined as:

$$\mathbf{v}_i = [[v(ux_1)_k, \dot{v}(x_1)_k], \ldots, [v(x_{N^f})_k, \dot{v}(x_{N^f})_k]]. \tag{30}$$

In the discrete case:

$$\mathbf{H}_k = \mathbf{H}_t, \qquad \mathbf{L}_k = \mathbf{L}_t, \qquad \mathbf{F}_k = e^{\mathcal{A}_t T_s}. \tag{31}$$

Subscript t denotes the temporal continuous model matrices in (20). The spectral density and the initialized state covariance have spatial structures as Eq.(22).

$$\mathbf{Q_k} = (\mathbf{P}_\infty - \mathbf{F}_k\mathbf{P}_\infty\mathbf{F}_k^\top), \quad \mathbf{P_0} = \mathbf{P}_{0,t}. \tag{32}$$

Based on this initial information and using the states and covariance and transition matrices in Eq.(28), we can predict the new state and covariance similar to a multi-variant Kalman filter. For sudo measurements $\mathbf{z_k(x_k)}$, Eq.(21) is used.

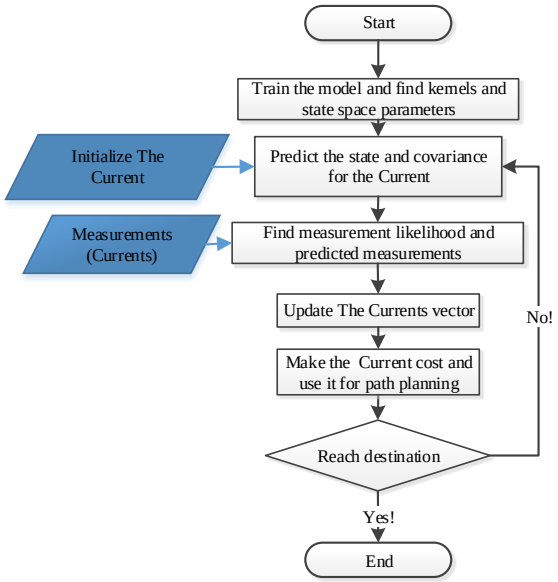

Fig. 3. General pipeline of tracking the ocean current in the USV path planning

$$\mathbf{v_{k+1|k}} = \mathbf{F_k v_{k|k}} \tag{33}$$
$$\mathbf{P_{k+1|k}} = \mathbf{F_k P_k F_k^\top} + \mathbf{Q_k}, \tag{34}$$
$$\upsilon_k = \mathbf{z_k} - \mathbf{H_k v_{k+1|k}}, \tag{35}$$
$$\mathbf{S_k} = \mathbf{H_k P_{k+1|k}} \boldsymbol{H_k^\top} \mathbf{R_k}, \tag{36}$$
$$\mathbf{K_k} = \mathbf{P_{k+1|k}} \bar{\mathbf{H}}_\mathbf{k}^\top \mathbf{S_k^{-1}}, \tag{37}$$
$$\mathbf{v_{k+1}} = \mathbf{v_{k+1|k}} + \mathbf{K_k}\upsilon_k, \tag{38}$$
$$\mathbf{P_{k+1}} = \mathbf{P_{k+1|k}} - \mathbf{K_k S_k K_k^\top}. \tag{39}$$

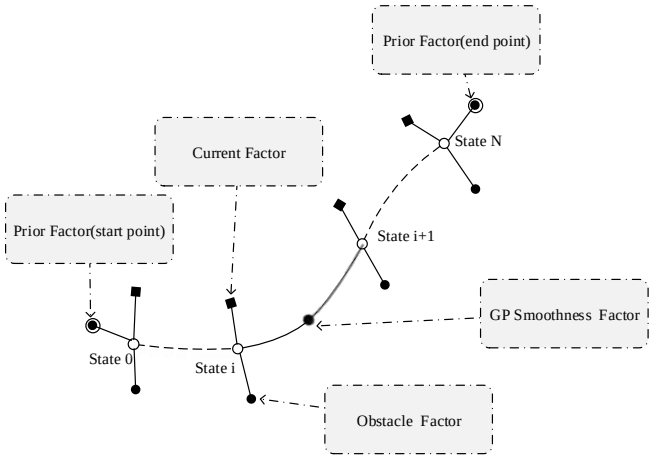

Fig. 4. A factor graph of a trajectory optimization problem for USV path planning. Note that the support states are marked as white circles, and there are four main types of factors, namely prior factors on the start and goal states, GP factors, Current factors, obstacle factors, and interpolation between states.

Algorithm 1. **Step tracking the Current**

Input: $\mathbf{Z_{k+1}}, \kappa(x, x'), \mathbf{x_k}, \mathbf{v_k}, \mathbf{P_k}$
Output: $\mathbf{v_{k+1}}, \mathbf{P_{k+1}}$ # The Current vector and Covariance

1: $\mathbf{F_k}, \mathbf{H_k}, \mathbf{Q_k}, \mathbf{R} \leftarrow$ Eq. 29 to 32
2: $\mathbf{v_{k+1|k}}, \mathbf{P_{k+1|k}} \leftarrow$ Eq. 33 and 34
3: $\mathbf{H}_k^f(\mathbf{x_k}) \leftarrow$ Eq. 27
4: $\mathbf{R}_k^f(\mathbf{x_k}) \leftarrow$ Eq. 26
5: $\boldsymbol{z_{k+1}}(\mathbf{x_k}) \leftarrow$ Eq. 24
6: $\mathbf{v_{k+1}}, \mathbf{P_{k+1}} \leftarrow$ Eq. 36 to 39
7: **return** $(\mathbf{v_{k+1}}, \mathbf{P_{k+1}})$

V. Simulation Scenario

A. Training the Model

We utilized a data set of the Halifax harbor ocean data from [26] [27]. Halifax Harbour is an estuary that is partly enclosed and heavily influenced by tidal patterns, wind activity, and various water discharges from sources such as the Sackville River, sewage systems, and coastal water distribution. The strongest Current in the harbor can reach speeds between 15-35 cm/s in the Narrows area and 5-15 cm/s along the boundary between the Inner and Outer Harbour. We employed distinct time and space kernels. Training was carried out using the Gpy Gaussian Process Python library and the Broyden-Fletcher-Goldfarb-Shanno (BFGS) optimization algorithm [28]. The outcome of the training process is a set of hyperparameters that can be applied to calculate the state space transition matrices. In the spatial domain, we trained and optimized the RBF kernel, similar to

Eq.(17), and in the temporal domain, the Matern kernel, equivalent to Eq. (25), using the training data $\{\mathbf{u}_d^*, \mathbf{z}_d^*\}_{d=1}^D$. The outcome of the training algorithm, Algorithm 2 is a set of transition variables in the time domain and an optimized kernel in the space domain. The optimized kernel, represented by $\hat{k}_x$, will be utilized to determine pseudo measurements and likelihoods in Eq.(24).

Algorithm 2. Training the Ocean Current Dynamics

Input: $\{\mathbf{x}_d^*, \mathbf{z}_d^*\}_{d=1}^D, \kappa(.), \sigma_0^2, l_0, \mathcal{T}$
Output: F, L, Qc, H, P_inf, P0

κ_t= Matérn (σ_0^2, l_0) #For the time domain
κ_x= RBF (σ_0^2, l_0) #In the space domain
$\mathrm{M_t} \leftarrow$ Gpy.GPRegression ($\{\mathbf{x}_d^*, \mathbf{z}_d^*\}_{d=1}^D, \kappa_t$)
$\mathrm{M_x} \leftarrow$ Gpy.GPRegression ($\{\mathbf{x}_d^*, \mathbf{z}_d^*\}_{d=1}^D, \kappa_x$)
$\hat{k}_t \leftarrow \mathrm{M_t}$.optimize('BFGS', max_iters)
$\hat{k}_x \leftarrow \mathrm{M_x}$.optimize('BFGS', max_iters)
$l, \sigma \leftarrow \hat{k}_t(l)$, $\hat{k}_t(\sigma)$ #Only for the time domain
$\lambda \leftarrow \sqrt{3}\tau/l$
$\mathrm{Q_c} \leftarrow 4\lambda^3\sigma^2$
$\mathcal{A}_t, \mathrm{L}_t, \mathrm{P}_\infty \leftarrow$ Eq. 31
$\mathrm{H}_k = \mathrm{H}_\mathcal{T}$, $\mathrm{L}_k = \mathrm{L}_\mathcal{T}$, $\mathrm{F}_k = e^{\mathcal{A}_\mathcal{T} T_s}, \mathrm{P}_0 = \mathrm{P}_\infty$
$\mathrm{Q_k} = \mathrm{P}_\infty - \mathrm{F_k P}_\infty \mathrm{F}^\top$
return $\mathrm{F}_k, \mathrm{L}_k, \mathrm{Q_k}$, H, P0, $\hat{k}_x$

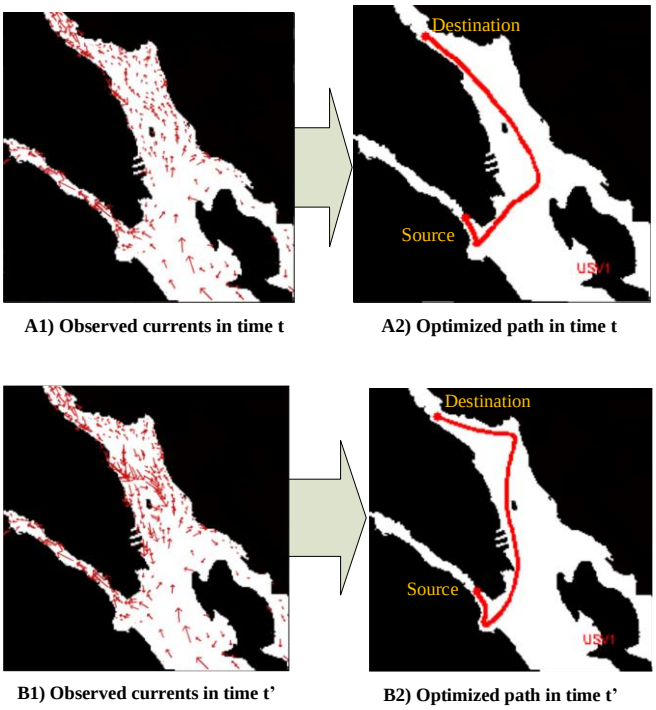

A1) Observed currents in time t
A2) Optimized path in time t
B1) Observed currents in time t'
B2) Optimized path in time t'

Fig. 5. Optimized path in two different times t and t' with different ocean currents.

B. USV path planning scenario

Let's consider a USV deployed for marine research and monitoring purposes in the Halifax area. Maps are created in the area with two longitudes and latitudes representing an area (-63.6177, 44.6745, -63.5037, 44.5978) as in Fig.2. The data used for the simulation and training of ocean currents are gathered from the sources referenced as [26] and [27]. The dataset comprises the hourly measurements of current velocity throughout a specific day. The goal is to determine the most optimal route for the USV to travel from its starting point to the destination. In this particular scenario, the USV is required to navigate through a complex maritime environment, which may consist of obstacles like islands, reefs, or shipping lanes. To evaluate the algorithm's performance, various ocean current scenarios were tested, and the corresponding paths were determined. Fig. 5 depicts the outcome when the current changes over time (t and t'). The path planning algorithm aims to ensure that the USV efficiently avoids collisions, and optimizes energy consumption. The initial step of the process involves creating a global path, which is then continuously refined and optimized at each trajectory step using relevant data sources, such as available maps, current measurements, and real-time sensor readings for localization. Based on this information, the algorithm generates a path that minimizes the cost of travel and the ocean current.

The resulting path involves waypoints as vector value functions where the USV needs to navigate between them while adapting to changing environmental conditions, as shown as the red paths in Fig. 5. The algorithm continuously localizes the position and updates the path during the mission to reach the destination.

As we can see in Fig.5A) and 5B), the path is adapting based on the change of the Current in time t and t' to minimize the consumption cost.

C. Comparison with AFM

In this section, we present a comparative analysis of our proposed method and a recently published study known as Anisotropic GPMP2 [6] across a real scenario. The Anisotropic GPMP2 approach incorporates AFM to construct a cost function for energy consumption. AFM is a numerical method extensively used in computational geometry and image processing to solve the Eikonal equation while considering the anisotropic characteristics of the environment. The Eikonal equation is a partial differential equation that describes the propagation of a wavefront through a medium with varying speeds. It calculates the time of arrival (or distance) from a given starting point to all other points in the domain by taking into account the varying speeds associated with each point. AFM, on its own, has the capability to be utilized for path planning, incorporating obstacle avoidance, and minimizing energy consumption. At each location, the local ocean current direction is mathematically represented as an anisotropy, and the energy measurement is determined to assign the highest importance to areas aligned with the ocean current direction. To calculate the cost of the Current in Anisotropic GPMP2, the following steps are needed:

Step 1: Make a grid from the environment and assign speeds or costs to each grid cell. Cells with higher costs represent areas where the USV will face more resistance or slower speeds.

Step 2: Apply the AFM algorithm to the grid with respect to the source and destination to compute the arrival times from the starting position to all other grid cells and use the result as the cost of the Current.

The utilization of AFM as a cost calculation method in vectorized regions is intriguing. However, the Anisotropic GPMP2 algorithm is susceptible to vulnerabilities based on three primary assumptions. Firstly, AFM assumes that the currents are part of the wavefront, which is not always true, especially in tidal areas. Secondly, in dynamic environments where the Currents constantly change, the algorithm necessitates updating the weights or speeds for each grid cell at every step, introducing potential vulnerabilities. Lastly, when consistent data is unavailable for the entire grid, the algorithm relies on interpolation, leading to computational difficulties, especially in large environments where interpolation must be performed for numerous grid cells. Another vulnerability emerges from the inherent characteristics of AFM and GPMP. AFM's reliance on the potential field of the environment with the destination introduces a potential bias when solely used for estimating current costs within GPMP. The path optimization in GPMP involves iterations to minimize the overall trajectory cost. However, in AFM, there is a possibility that points closer to the destination will consistently have lower costs compared to those closer to the source, which can potentially distort the estimation, Fig. 6.

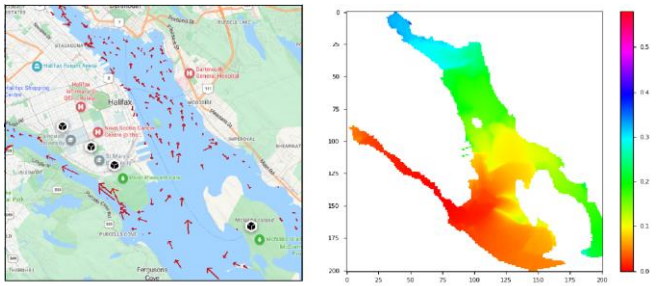

(A) (B)

Fig. 6. (A) Given ocean currents; (B) AFM arrival time based on the linear interpolation of currents and source. It also showing a noticeable bias in the points near the source point in (B).

We conducted a comparison between our algorithm and Anisotropic GPMP2 to demonstrate the impact of bias. The scenario mentioned in Fig. 6 was used for testing. Both algorithms utilized RRT* [13] for generating the initial path. The current information was obtained from the datasets in [26] and [27], and the same arguments were applied to both algorithms. The main difference lies in how trajectory costs were computed. Our algorithm tracked the current using GP, while Anisotropic GPMP2 used AFM. The results are presented in Fig. 7. In Fig. 7, it is evident that points closer to the source have lower costs due to the characteristics of AFM, causing wavering in GPMP2 compared to our algorithm, which independently computed the cost for each point along the trajectory.

VI. Conclusions

This study presents a pioneering approach aimed at tracking the vector of energy consumption during movement. It improves upon the GPMP2 model by incorporating a novel spatiotemporal factor, which enables the tracking and prediction of ocean currents using spatiotemporal Gaussian process inference. To validate the effectiveness of the proposed method, experiments were conducted in the demanding environment of Halifax Harbor, specifically targeting the tracking of ocean currents.

As a direction for future research, it would be worthwhile to expand the scope of the model by incorporating additional factors that influence energy consumption, such as water density and wind. By considering these additional factors, the model could offer a more comprehensive understanding of the energy dynamics involved.ss

The developed methodology holds promise for diverse applications in oceanic studies. Notably, it enables simultaneous tracking of both the path and the currents within the ocean. This opens up possibilities for further investigations and studies in related fields, demonstrating the potential significance of this method in shaping future research endeavors.

.

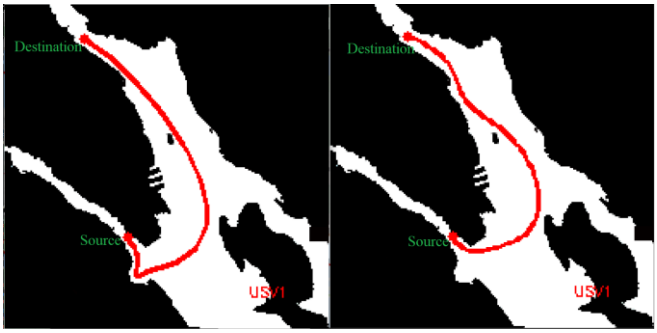

(A) Proposed Algorithm (B)Anisotropic GPMP2

Fig. 7. Path planning for the scenario depicted in Fig. 6. It points out in (B) that in Anisotropic GPMP2, due to a bias, the lower costs assigned to points near the source lead to the unmanned surface vehicle (USV) passing through higher currents.

Acknowledgment

This work was supported in part by the MITACS Accelerate program of the project named “Intelligent Unmanned Surface Vehicles with Safe Navigation and Docking in Harsh Marine Environment” in collaboration with Marine Thinking Inc, Canada, and the Natural Sciences and Engineering Research Council, Canada.

References

[1] J. Dong, M. Mukadam, F. Dellaer and B. Boots, "Motion planning as probabilistic inference using Gaussian processes and factor graphs," in *Proceedings of Robotics: Science and Systems*, Stockholm, Sweden, may 16-21, 2016.

[2] M. Mustafa, D. Jing, Y. Xinyan, D. Frank and B. Byron, "Continuous-time Gaussian process motion planning via probabilistic inference," *arXiv*, 2018.

[3] S. Wang, M. Fu, Y. Wang and L. Zhao, "A Multi-Layered Potential Field Method for Water-Jet Propelled Unmanned Surface Vehicle Local Path Planning with Minimum Energy Consumption," *Polish Maritime Research*, vol. 26, no. 1, pp. 134-144, March 2019.

[4] R. Song, Y. Liu and R. Bucknall, "A multi-layered fast marching method for unmanned surface vehicle path planning in a time-variant maritime environment," *Ocean Engineering*, vol. 129, no. 0029-8018, pp. 301-317, 2017.

[5] R. Song, Y. Liu, W. Liu and R. Bucknall, "A Two-layered Fast Marching Path Planning Algorithm for an Unmanned Surface Vehicle Operating in a Dynamic Environment," in *OCEANS*, Genova, Italy, 2015.

[6] J. Meng, Y. Liu, R. Bucknall, W. Guo and Z. Ji, "Anisotropic GPMP2: A Fast Continuous-Time Gaussian Processes Based Motion Planner for Unmanned Surface Vehicles in Environments With Ocean Currents," *IEEE TRANSACTIONS ON AUTOMATION SCIENCE AND ENGINEERING*, vol. 19, no. 4, pp. 3914-3931,, Oct. 2022.

[7] Y. Singh, S. Sharma, R. Sutton, D. Hatton and A. Khan, "A constrained A* approach towards optimal path planning for an unmanned surface vehicle in a maritime environment containing dynamic obstacles and ocean currents," *Ocean Engineering*, vol. 169, pp. 187-201, December 2018.

[8] A. Topaj, O. Tarovik, A. Bakharev and A. Kondratenko, "Optimal ice routing of a ship with icebreaker assistance," *Applied Ocean Research*, vol. 86, pp. 177-187, May 2019.

[9] P. E. Hart, N. J. Nilsson and B. Raphael, "A formal basis for the heuristic determination of minimum cost paths," *IEEE transactions on Systems Science and Cybernetics*, vol. 4, no. 2, pp. 100-107, 1968.

[10] L. E. Kavraki, P. Svestka, J. C. Latombe and M. H. Overmars, " Probabilistic roadmaps for path planning in high-dimensional configuration spaces," *IEEE transactions on Robotics and Automation*, vol. 12, no. 4, pp. 566-580, 1996.

[11] S. M. LaValle, " Rapidly-exploring random trees: A new tool for path planning," Technical Report. Computer Science Department, Iowa State University, 1998.

[12] J. J. Kuffner and S. M. LaValle, " RRT-connect: An efficient approach to single-query path planning," in *2000 ICRA. Millennium Conference. IEEE International Conference on Robotics and Automation. Symposia Proceedings* , April 2000.

[13] S. Karaman and E. Frazzoli, "Sampling-based algorithms for optimal motion planning.," *The international journal of robotics research*, vol. 30, no. 7, pp. 846-894, 2011.

[14] C. E. Rasmussen and C. K. I. Williams, Gaussian Processes for Machine Learning, MIT Press, 2006.

[15] M. Mustafa, Y. Xinyan and B. Byron, "Gaussian Process Motion Planning," in *Proc. IEEE Conference on Robotics and Automation (ICRA-2016)*, 2016.

[16] J.-S. Ha, H.-J. Chae and H.-L. Choi, "Approximate Inference-Based Motion Planning by Learning and Exploiting Low-Dimensional Latent Variable Models," *IEEE ROBOTICS AND AUTOMATION LETTERS*, vol. 3, no. 4, pp. 3892-3899, October 2018.

[17] C. E. Rasmussen and C. K. Williams, Gaussian processes for machine learning, 1st Edition ed., MIT Press, Cambridge, 2006.

[18] C. H. Tong, P. Furgale and T. D. Barfoot, "Gaussian Process Gauss–Newton for non-parametric simultaneous localization and mapping.," *The International Journal of Robotics Research*, vol. 32, no. 5, p. 507–525, 2013.

[19] M. Mustafa, D. Jing, Y. Xinyan, D. Frank and B. Byron, "Continuous-time Gaussian process motion planning via probabilistic inference," *arXiv*, 2018, https://arxiv.org/abs/1707.07383.

[20] S. Anderson, T. D. Barfoot, C. H. Tong and S. Särkkä, "Batch Continuous-Time Trajectory Estimation as Exactly Sparse Gaussian Process Regression," *Autonomous Robots*, vol. 39, no. 3, pp. 221-238, July 2015.

[21] M. Kaess, H. Johannsson, R. Roberts, V. Ila, J. Leonard and F. Dellaert, "iSAM2: Incremental Smoothing and Mapping Using the Bayes Tree," *The International Journal of Robotics research.*, vol. 31, no. 2, pp. 216-235, May 2012.

[22] W. Aftab, R. Hostettler, A. D. Freitas, M. Arvaneh and L. Mihaylova, "Spatio-temporal gaussian process models for extended and group object tracking with irregular shapes.," *IEEE Transactions on Vehicular Technology*, p. 68(3):2137–2151, March 2019.

[23] N. Wahlstrom and E. Ozkan, "Extended target tracking using Gaussian processes," *IEEE Transactions on Signal Processing*, vol. 63, p. 4165–4178, 2015.

[24] S. Särkkä, A. Solin and J. Hartikainen, "Spatiotemporal Learning via Infinite-Dimensional Bayesian Filtering and Smoothing: A Look at Gaussian Process Regression through Kalman Filtering," *IEEE Signal Processing Magazine*, vol. 30, pp. 51-61, July 2013.

[25] D. Wang, J. Xue, D. Cui and Y. Zhong, "A robust submap-based road shape estimation via iterative Gaussian process regression," *2017 IEEE Intelligent Vehicles Symposium (IV)*, pp. 1776-1781, 2017.

[26] S. Shan, "Numerical Study of Three-dimensional Circulation and Hydrography in Halifax Harbour Using a Nested-grid Ocean Circulation Model," 21 12 2010. [Online]. Available: http://hdl.handle.net/10222/13173.

[27] D. A. Greenberg, T. S. Murty and A. Ruffman, "A numerical model for the Halifax harbor tsunami due to the 1917 explosion," *Marine Geodesy*, vol. 16, no. 2, pp. 153-167, 1993.

[28] R. Fletcher, Practical Methods of Optimization, 2nd ed. ed., New York: John Wiley & Sons, 1987.

[29] X. Pan, J. Shi, P. Luo, X. Wang and X. Tang, " Spatial as deep: Spatial cnn for traffic scene understanding," *Computer Vision and Pattern Recognition(cs.CV)*, p. arXiv:1712.06080, Dec 2017.

Behzad Akbari , a member of IEEE, obtained his bachelor's and master's degrees in computer software and computer architecture from Tehran and Knowledge And Research University, Iran, in 1996 and 1999 respectively. He later completed his second master's and PhD degrees in Computer Science and Electrical and Computer Engineering (ECE) from McMaster University, Canada, in 2014 and 2021 respectively. Currently, he holds a postdoctoral fellowship at Dalhousie University, Halifax, Nova Scotia, Canada, in the Department of Mechanical Engineering. He has editorial experience with IEEE Access, Transactions on Robotics, and Transactions on Systems, Man and Cybernetics (SMC). His research focuses on state estimation algorithms, collaborative multi-agent systems, multi-target tracking, multi-output Gaussian process, iterative localization and mapping, factor graph optimization, and reinforcement learning.

Ya-Jun Pan (S'00-M'03-SM'11) is a Professor in the Dept. of Mechanical Engineering at Dalhousie University, Canada. She received the B.E. degree in Mechanical Engineering from Yanshan University, the M.E. degree in Mechanical Engineering from Zhejiang University, and the Ph.D. degree in Electrical and Computer Engineering from the National University of Singapore. She held post-doctoral positions of CNRS in the Laboratoire d'Automatique de Grenoble in France and the Dept. of Electrical and Computer Engineering at the University of Alberta in Canada respectively. Her research interests are robust nonlinear control, cyber physical systems, intelligent transportation systems, haptics, and collaborative multiple robotic systems. She has served as Senior Editor and Technical Editor for IEEE/ASME Trans. on Mechatronics, Associate Editor for IEEE Trans. on Cybernetics, IEEE Transactions on Industrial Informatics, IEEE Industrial Electronics Magazine, and IEEE Trans. on Industrial Electronics. She is a Fellow of Canadian Academy of Engineering (CAE), Engineering Institute of Canada (EIC), ASME, CSME, and a registered Professional Engineer in Nova Scotia, Canada.

Shiwei Liu is Marine Thinking's CTO, who is experienced in developing products for the marine sector with AI and machine learning technologies. He holds a master's degree in computer science from the University of Utah and has over 12 years of experience in Machine Learning, Artificial Intelligence, and Software Engineering fields. Before joining Marine Thinking in 2019, he was a Senior Data Scientist at Vivint Smart Home and led a team of data scientists and engineers to deliver an innovative world-class home security AI solution to clients. He has been granted over 10 US patents, and many others internationally, particularly in Canada and Europe. At Marine Thinking, Shiwei critically evaluates potential projects and makes high-level decisions on their technical feasibility. He is also responsible for technical product planning, leading project teams, and communicating with employees, stakeholders, and customers.

Tianye Wang is an AI-Software Lead at Marine Thinking, He received his bachelor's degree and master's degree in computer science from Dalhousie University, Canada. In his role, he leads a team of experts and collaborates with research institutions such as the National Research Council (NRC) and MITACS responsible for developing AI autopilot system for uncrewed surface vehicles (USVs) and machine learning-based solutions on edge devices for the marine sector. His research interests are computer vision, deep learning, edge computing, sensor fusion, autonomous navigation and mapping, swarm robotics, and machine-learning security.